LA-UR- 97-4773

CONF-970710--

ELECTRON COLLISIONS WITH COHERENTLY PREPARED ATOMIC TARGETS

S. TRAJMAR, I. KANIK, L. R. LeCLAIR and M. A. KHAKOO
Jet Propulsion Laboratory, California Institute of Technology
4800 Oak Grove Dr., Pasadena, CA 91109, USA

I. BRAY and D. FURSA
Electronic Structure of Materials Centre, The Flinders University of South Australia,
P. O. Box 2100, Adelaide 5001, Australia

G. CSANAK
Los Alamos National Laboratory, University of California,
Los Alamos, NM 87545, USA

RECEIVED
MAR 2 5 1998
OSTI

The subject of electron scattering by laser-excited atoms is briefly reviewed. To demonstrate some aspects of these electron collision processes, we describe the procedures and the results of a joint experimental and theoretical study concerning elastic scattering by coherently excited ^{138} Ba (...6s6p $^1P_1$) atoms. Examples of experimental and theoretical collision parameters and magnetic sublevel differential cross sections for elastic scattering are given and compared. The convergent close coupling calculations (with the neglect of spin-orbit interaction) are in good agreement with experiment at 20 eV impact energy and 10, 15 and 20° scattering angles and can be expected to yield reliable integral magnetic sublevel and alignment creation cross sections. The role of these quantities in plasma polarization spectroscopy is pointed out.

19980422 086

1 Introduction

Extensive cross section data base is available for electron collision processes involving ground state atoms. The same, however, cannot be said for electron collisions with excited species. The main reason for this has been the difficulty that one encounters in trying to produce atoms in specific excited states with sufficiently high density for such studies. The various techniques for preparation of excited atoms and a summary of the available electron collision data for these atoms were reviewed by Lin and Anderson[1] and Trajmar and Nickel[2].

With the utilization of lasers for preparing the excited atoms, many of the difficulties encountered previously disappear but some aspects of the laser excitation process, like coherence and polarization, enter the electron collision process.

DISTRIBUTION OF THIS DOCUMENT IS UNLIMITED

MASTER

DTIC QUALITY INSPECTED 4

A few general remarks on laser excitation of atoms and on the subsequent electron scattering processes are appropriate here. The important characteristics of laser excitation are:

(a) ***Selectivity***.The typical 10^{-9} eV energy resolution, associated with the laser, allows us to excite specific fine, hyperfine levels and/or isotopic species.

(b) ***Polarization***. The polarized nature of laser light allows us to prepare polarized (aligned or oriented) atomic ensembles with full control over the magnetic sublevel populations.

(c) ***Coherence***. The coherence of the laser light is transferred to the atoms in the excitation process. The state of the excited atoms is a coherent superposition of the magnetic sublevel states and the whole atomic ensemble is coherently prepared. The coherent state is determined by the laser geometry and polarization.

(d) ***High power density***. The high power density of the laser beam makes possible the generation of large excited state population fractions both in the state directly excited by the laser and in lower lying metastable states populated by cascade processes.

All these good characteristics of laser excitation come, however, with some strings attached. The experimental procedures themselves as well as the interpretation of the experimental results become more complicated:

(a) The cross sections become, in general, dependent on the azimuthal scattering angle (or equivalently on the laser beam incident angles with respect to the collision frame).

(b) The polarization and coherence characteristics of the target atoms need to be fully specified in order to precisely define the cross section in question and to make comparisons between experiment and theory meaningful.

(c) The population fraction for the ground and excited species in the mixed target beam have to be determined in order to be able to convert the measured scattering intensities to the corresponding cross sections.

The first application of laser excitation in electron scattering measurements was introduced in the early 1970's by Hertel and coworkers for Na[3]. Shortly after that, we initiated our work on Ba[4]. Since then measurements have been carried out on Li, K, Rb, Mg, Ca, Cr and Yb[5,6]. In most of these studies, the superelastic scattering signal corresponding to the deexcitation of the laser prepared state to the ground state was measured as a function of laser polarization and incident angles. The results were then interpreted in terms of the electron impact coherence parameters (EICP's) for the hypothetical "inverse" inelastic scattering process. This "inverse" process corresponds to electron impact excitation of the isotropic,

DISCLAIMER

This report was prepared as an account of work sponsored by an agency of the United States Government. Neither the United States Government nor any agency thereof, nor any of their employees, makes any warranty, express or implied, or assumes any legal liability or responsibility for the accuracy, completeness, or usefulness of any information, apparatus, product, or process disclosed, or represents that its use would not infringe privately owned rights. Reference herein to any specific commercial product, process, or service by trade name, trademark, manufacturer, or otherwise does not necessarily constitute or imply its endorsement, recommendation, or favoring by the United States Government or any agency thereof. The views and opinions of authors expressed herein do not necessarily state or reflect those of the United States Government or any agency thereof.

noncoherent ground state to the upper state. The interpretation is based on the theory of Macek and Hertel[7]. The EICP's fully characterize the excited state, allow us a much deeper insight into the nature of electron-atom collisions, and present a more rigorous check for theoretical calculations than cross sections derived from conventional scattering measurements. Some results have also been reported on stepwise excitation process[5,6]. The results of these efforts have been extensively discussed in the literature and at the Coherence and Correlation Symposia associated with the ICPEAC's, therefore, this topic is not discussed any further here.

No studies similar to the superlastic measurements have been reported until now for elastic electron scattering by laser-excited atoms. We will concentrate here on this topic to demonstrate some aspects and characteristics of electron scattering by coherently excited atomic ensembles. Specifically, we will discuss excitation of ^{138}Ba ...6s^2 ^{1}S$_0$ atoms to the ...6s6p ^{1}P$_1$ state using in-plane, linearly polarized laser light and the subsequent study of elastic scattering process by these excited atoms. It should be mentioned for completeness that some elastic and inelastic scattering cross sections have been extracted for oriented Na ($3^2P_{3/2}$, F=3, $M_F = \pm 3$) atoms from atomic recoil measurements by Vuskovic and coworkers[8].

2 Electron scattering by laser-excited ^{138}Ba(...6s6p ^{1}P$_1$) atoms

2.1 Background

The selection of Ba for our studies was originally dictated by the availability of the appropriate laser. As it turned out, ^{138}Ba was also a good choice because of its simple energy level scheme. Laser excitation from the ground ^{1}S$_0$ state to the ^{1}P$_1$ level can be conveniently achieved. The ^{1}P$_1$ level has no fine or hyperfine structure and is well separated from other isotopic levels. Note also that cascade processes can build up significant populations in the ^{1}D$_2$ and ^{3}D$_2$ metastable levels and electron collision processes with these species can also be studied.

2.2 Experimental arrangement and procedures

The experimental arrangement is shown schematically in Fig. 1. A nearly monoenergetic ($\Delta E_{1/2} \sim 50$ meV) electron beam comes along the Z_{coll} axis, crosses the target Ba beam at 90° and scatters by polar angles θ, ϕ with respect to the original direction. The spin of the incoming and outgoing electrons is not determined. The initial and final momenta of the electrons define the collision

plane (Z_{coll} X_{coll}). The Ba beam propagates along the Y_{coll} axis. It is collimated and contains all naturally occuring isotopes. We will be concerned here only with the 138 isotope which is about 72% of the mixture. The laser beam is in the scattering plane and its direction with respect to the laboratory frame (which is the same as the collision frame for scattering to the left) is defined by the polar angles θ_v, ϕ_v. It is linearly polarized and the angle of the polarization with respect to the scattering plane is denoted by ψ. For details see ref. 4b. With this arrangement we studied the scattering signal as a function of the energy lost (ΔE) by the electron (at fixed E_o, θ; θ_v, ϕ_v and ψ) or as a function of ψ (at fixed E_o, θ; θ_v, ϕ_v and ΔE). The first case yields the energy-loss spectra and the second one yields the intensity modulation curves.

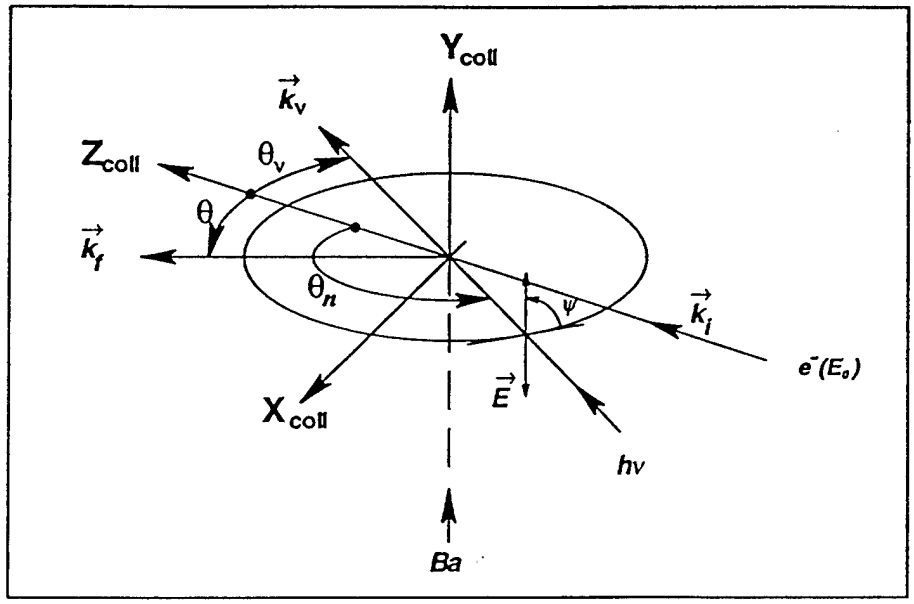

Figure 1: Schematic diagram for the experimental arrangement. See text for explanation.

The energy-loss spectra contain features corresponding to excitation of the ground and laser-excited atoms, deexcitation of the laser-excited and cascade-populated metastable atoms and to elastic scattering by all these species. We could study the polarization dependence of the scattering signal in any of these channels, but here we concern ourselves only with elastic scattering.

2.3 *Theoretical calculations*

Parallel with the experimental efforts, we calculated scattering amplitudes associated with elastic and several inelastic channels for coherently excited $^{138}Ba(^1P_1)$ atoms. In these calculations the first order manybody theory (FOMBT) and the unitarized distorted wave approximation (UDWA) were used for inelastic scattering[9,10a,10b] and the convergent close coupling (CCC) method was used along with the LS-coupling scheme for both elastic and inelastic[10a,10b] scattering. Theoretical results and comparisons with experiment will be shown for the elastic case.

2.4 *Elastic scattering by $^{138}Ba(...6s6p\ ^1P_1)$ atoms*

These scattering studies were motivated partly by the lack of collision parameters and cross sections for elastic electron collisions with coherently excited atoms and partly by the question raised in connection with plasma polarization spectroscopy as to whether elastic electron collisions can generate alignment and to what degree.

We measured the total elastic scattering signal as a function of ψ (for fixed E_0, θ, θ_v, ϕ_v and $\Delta E=0$). The total signal consists of contributions from background , from elastic scattering by ground state atoms of all isotopes, from elastic scattering by metastable ^{138}Ba atoms and finally from elastic scattering by the coherently excited ^{138}Ba ($^1P_1$) atoms [$I_{cP}(\psi)$]. We are really interested in the last contribution and, therefore, the other contributions had to be determined and subtracted out. The next step in the evaluation procedure is to convert the modulation signal [$I_{cP}(\psi)$] to the corresponding differential cross section [$DCS_{cP}(\psi)$]. Normalization to the absolute scale was obtained from the ratio of $I_{cP}(\psi)$ to the ($^1S_0 \rightarrow {}^1P_1$) inelastic signals with the utilization of the known cross sections for the ($^1S_0 \rightarrow {}^1P_1$) process[11].

The result of all these manipulations is the cross section modulation curve which is given as

$$DCS_{cP}(\psi) = A^{Exp} + B^{Exp} \cos 2\psi = 3/4\ DCS_P \{A + B \cos 2\psi\},$$

where DCS_P is the magnetic sublevel averaged (incoherent averaging) elastic differential scattering cross section for ^{138}Ba ($^1P_1$) atoms. A and B were determined by a least square fitting procedure. They contain geometrical factors associated with the laser and parameters related to the physics of the electron collision process. To

be able to extract these parameters, we needed to generate modulation equations with at least two laser geometries. In order to improve on statistical errors and checks, we produced modulation curves with four laser geometries (θ_v =45° and 90° and both with ϕ_n = 0° and 180°) for each E_0, θ case. To be able to do the subtractions, normalizations and various check measurements and to generate four modulation equations, we had to carry out 116 measurements at each E , θ case.
The modulation equations can be interpreted by two different schemes:
(i) In terms of EICP's associated with the hypothetical "inverse" process:
^{138}Ba ($^1P_1$, M_i = isotr.,incoh.) + e (E_0) → ^{138}Ba ($^1P_1$, M_f = coh.,align.) + e (E_0)
(ii) In terms of parameters associated with the actual experimental ("forward") process:
^{138}Ba ($^1P_1$, M_i = coh 0±1) + e (E_0) → ^{138}Ba ($^1P_1$, M_f = undet.) + e (E_0).
In the case, which we are discussing here, both processes are elastic scattering processes.

In the first evaluation scheme the modulation equations are evaluated with

$$A = 1+\cos^2\theta_n + \lambda(1-3\cos^2\theta_n) + (\lambda-1)\cos\varepsilon(1+\cos^2\theta_n) + k\sin 2\theta_n\cos\phi_n,$$

$$B = (3\lambda-1)\sin^2\theta_n + (1-\lambda)\cos\varepsilon(1+\cos^2\theta_n) + k\sin 2\theta_n\cos\phi_n,$$

where $k = 2\sqrt{\lambda(1-\lambda)}\cos\Delta\cos\tilde{\chi}$ and

$\theta_n = \theta_v + \theta\cos\phi_n$ and $\phi_n = \phi_v - \pi = 0°$ ($\phi_n = \phi_v = 180°$) for scattering to the left (right).

Here the factors associated with the laser geometry (θ_n, ϕ_n) and the four EICP's (λ, cos ε, cos Δ and $\tilde{\chi}$) are explicitly shown. The definitions of θ_n and ϕ_n assure that the EICP's (and magnetic sublevel cross sections derived from them) are referred to the collision frame associated with the "inverse" process; that is the reference direction, is taken along the momentum vector of the incoming electron for this "inverse" process. The EICP's (dropping the P index) are defined as:

$$\lambda = \frac{DCS(M_f=0)}{DCS},$$

$$\cos\varepsilon = -\frac{\frac{1}{3}\sum_{M_i} f(M_i, M_f=1).f^*(M_i, M_f=-1)}{DCS(M_f=1)},$$

$$\cos\Delta = \frac{\frac{1}{3}\sum_{M_i}\left|f(M_i, M_f=1).f^*(M_i, M_f=0)\right|}{\sqrt{DCS(M_f=1)DCS(M_f=0)}}$$

and $\cos\tilde{\chi} = \cos\{\arg[\frac{1}{3}\sum_{M_i} f(M_i, M_f = 1).f^*(M_i, M_f = 0)]\}$.

The convention we use here is that averaging over omitted quantum numbers is implied.

E.g. $DCS(M_f = 0) = \frac{1}{3}\sum_{M_i} DCS(M_i, M_f)$

and $DCS = \frac{1}{3}\sum_{M_i}\sum_{M_f} DCS(M_i, M_f)$.

The EICP's characterize the state prepared by the "inverse" electron collision process. (They are equivalent to the density matrix of this state). For example, cos ε corresponds to the off-diagonal matrix element representing the M_i averaged interference between the f (M_i, M_f = 1) and f (M_i, M_f = -1) scattering amplitudes. From the present experiments we can extract only λ, cos ε and k.

In Figure 2, λ and cos ε are shown for E_0 = 20 eV. The curves correspond to our results from the CCC calculations and the symbols with the error bars are from the experiments. The agreement between theory and experiment is excellent for λ and close for cos ε.

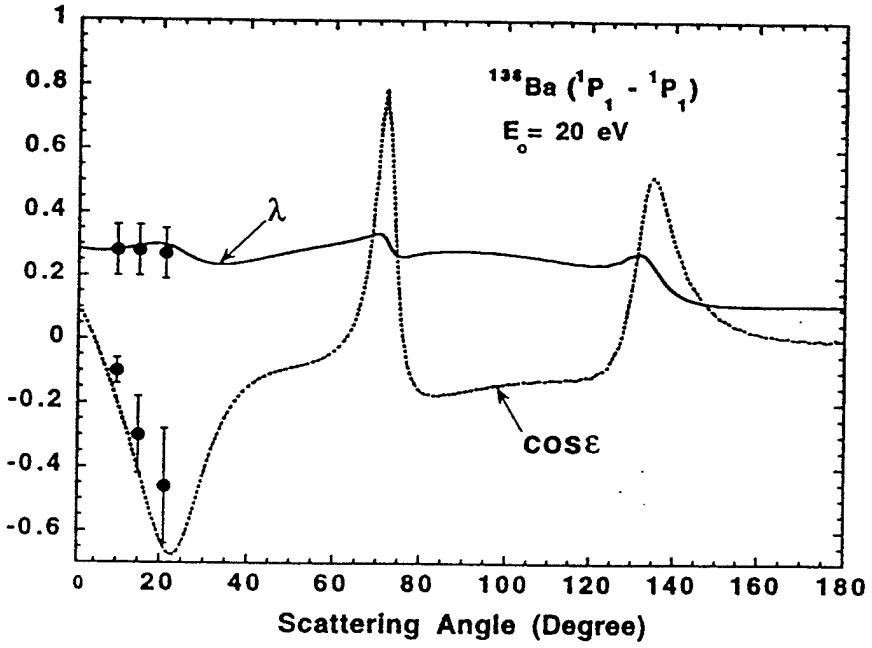

Figure 2: The EICP's, λ and cos ε at E_0 = 20 eV, solid and dotted curves, respectively. The experimental values are indicated by filled circles with error bars.

The discrepancy for cos ε may be due to spin-orbit coupling effect, which was neglected in the calculations, and the deviation in the theoretical values from unity (which would correspond to full coherence) is strictly due to averaging over M_i.

From the EICP's and DCS (which was also determined in our experiments), we obtained the DCS (M_f= 0) and DCS (M_f = 1) = DCS(M_f= -1) values. These results are shown and compared with the theoretical results in Fig. 3. The various cross sections show similar angular behavior with deep minima at around 72° and at around 135°. They are also similar in absolute value. Calculations show that the DCS (M_i, M_f) values deviate from each other by more than an order of magnitude but these differences are eliminated, to a large extent, in the averaging process. The differences in the DCS (M_f= 1) and DCS (M_f = 0) values, which determine the alignment creation cross section, are not negligible at most scattering angles. This matter will be discussed later.

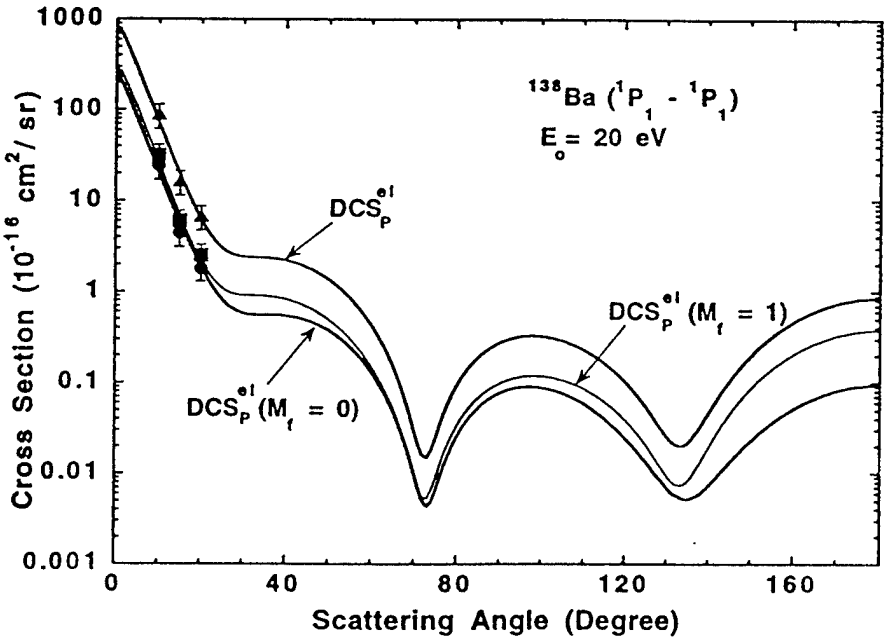

Figure 3: Differential elastic scattering cross sections at E_0 = 20 eV. See text for explanations of symbols.

In the second evaluation scheme, we interpret the modulation equation in terms of collision parameters associated with the actual ("forward") scattering process. This

evaluation scheme is similar to that used for the inverse process but now we refer the collision parameters and the magnetic sublevel cross sections to the collision frame associated with the "forward process". Here $\theta_n = \pi - \theta_v$ and $\phi_n = \phi_v - \pi = 0°$ ($\phi_n = \phi_v = 180°$) for scattering to the left (right). The collision parameters (p_1, p_2, p_3 and p_4) have different meanings than the EICP's. Here the coherence was created by the laser excitation and no magnetic sublevel information is available for the final state. We can again extract only p_1, p_2 and $h = 2\sqrt{p_1(1-p_1)}p_3 p_4$. These parameters are very useful because from them we can generate cross sections, $DCS_{cP}(\theta_n, \phi_n, \psi)$, for elastic scattering by atoms prepared by any laser geometry and polarization or equivalently by atoms in any coherent superposition state of the magnetic sublevels, DCS (M_i = coh 0, ± 1) = $\sum_{M_f} |\sum_{M_i} C_{M_i} f(M_i, M_f)|^2$. Here C_{M_i} is the complex coefficient in the superposition of the laser prepared coherent initial state wave function in terms of the magnetic sublevel wave functions.

The azimuthal asymmetry of elastic scattering (left/right scattering asymmetry) can be given by the collision parameters as:

$$A = \frac{DCS_{cP}(\theta_n, \phi_n = 0^0, \psi) - DCS_{cP}(\theta_n, \phi_n = 180^0, \psi)}{DCS_{cP}(\theta_n, \phi_n = 0^0, \psi) + DCS_{cP}(\theta_n, \phi_n = 180^0, \psi)}$$

$$= \frac{2\sqrt{p_1(1-p_1)}p_3 p_4 \sin 2\theta_n (1+\cos 2\psi)}{1+\cos^2\theta_n + p_1(1-3\cos^2\theta_n) + (p_1 - 1)p_2 \sin^2\theta_n + \alpha} ,$$

where $\alpha = [(3p_1 - 1)\sin^2\theta_n + (1-p_1)p_2(1+\cos^2\theta_n)]\cos 2\psi$.

The asymmetry for the case of $\theta_v = 45°$ and $\psi = 0°$ is shown in Fig. 4.

It should be noted that the EICP's and the collision parameters are, in principle, related. Also, if one set of parameters is known, we can generate the modulation equations and analyze them in terms of the other set of parameters.

Comparison of the experimental and calculated parameters and cross sections gives good agreement at $E_0 = 20$eV and scattering angles of 10, 15 and 20°. We can therefore rely, with some confidence, on the theoretical results over the full angular range and generate integral cross sections. These cross sections as well as cross sections at two other energies are shown in Table 1. Also shown in this table are the alignment creation cross sections which are defined as[12]

$$Q_{CR}^{[2]} = \sqrt{\tfrac{2}{3}}[Q(M_f = 1) - Q(M_f = 0)].$$

Table 1: Summary of integral cross sections for Ba from CCC calculation (in 10^{-16} cm^2 units).

($^1P_1$ - $^1P_1$) elastic	2.8 eV	20.0 eV	98.0 eV
Q (1, 1)=Q (-1,-1)	119.64	36.62	18.07
Q (1, 0)=Q (-1, 0)	1.97	0.74	0.054
Q (1,-1)=Q (-1,-1)	4.62	1.57	0.37
Q (0, 1)=Q (0,-1)	1.16	0.62	0.054
Q (0, 0)	89.33	28.54	14.75
Q (M_i= 0)	91.65	29.79	14.85
Q (M_i=1)= Q (M_i= -1)	126.24	38.91	19.02
Q (M_f= 0)	31.09	10.01	4.[illegible]
Q (M_f= 1)= Q (M_f= -1)	41.81	12.93	6.16
Q	114.71	35.87	17.28
$Q^{[2]}_{CR}$ =(2/3)$^{1/2}$[Q(M_f=1)-Q(M_f=0)]	8.74	2.88	0.99
($^1S_0$ - $^1S_0$) elastic			
Q (0,0) = Q	CCC (E_o=22.2 eV)	28.16	
Q	Exp* (E_o=20.0 eV)	26.7	

*Wang et al. J. Phys. B 27, 1613 (1994).

These cross sections are important parameters in plasma polarization spectroscopy and although they are about an order of magnitude smaller than some of the other integral cross sections they are, by no means, negligible.

3 Plasma Polarization Spectroscopy (PPS)

In this last section, we are going to point out briefly how the magnetic sublevel scattering cross sections enter PPS.

The information contained in the polarization of radiation emitted by various plasmas has not been fully utilized so far. This was, to a large extent, due to the lack of appropriate equations which relate the observed polarization to the local plasma conditions. In recent years, a great deal of progress was made in

deriving and utilizing these equations (See ref.12). In many plasma systems the polarization of the atomic constituents of the plasma (and therefore of the emitted radiation) is due to the anisotropy of the electron flux. For such cases magnetic sublevel electron impact cross sections enter the equations as parameters and are needed for the evaluation of the observations. Very little cross section data of this type exist at the present time from experiments. Although theoretical calculation could, in principle, supply such data, one needs to check the results of the calculations against benchmark measurement to asses their reliability. The experiments and calculations described here were steps in this direction. The emphasis was put first on elastic scattering since there were questions raised as to whether it can create alignment. Our studies answered this question in general. It should be noted that the diagnostic species do not have to be a natural component of the plasma but could be trace elements introduced for this purpose, e.g., Ba which has been used for such purpose in the past.

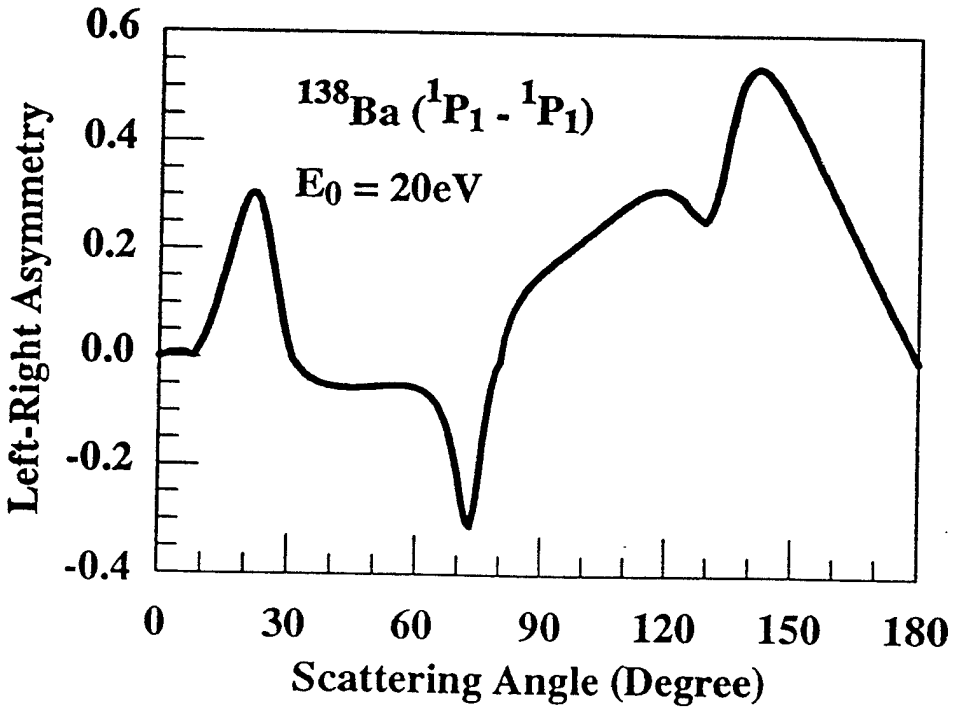

Figure 4: The values of the left-rigth scattering asymmetry parameters for $\theta_v = 45°$ and $\psi = 0°$.

Acknowledgments

Valuable discussions with T. Fujimoto, S. A. Kazantsev and D.C. Cartwright are acknowledged.

References

1. C. C. Lin and W. Andersen, Advances in Atomic, Molecular and Optical Physics 29, 1 (1992).
2. S. Trajmar and J. C. Nickel, Advances in Atomic, Molecular and Optical Physics, 30, 45 (1992).
3. I. V. Hertel and W. Stoll, J. Phys. B. 7, 583 (1974).
4a. D. F. Register, S. Trajmar, G. Csanak, S. W. Jensen, M. A. Fineman and R. T. Poe, Phys. Rev. A28, 151 (1983); 4b. P. W. Zetner, S. Trajmar and G. Csanak, Phys. Rev. A41, 5980 (1990).
5. Canadian J. Phys., 74, 977-996, (1996).
6. Internat. Symp. on Polarization and Correlation in Electronic and Atomic Collisions, Frascati, Italy, July31 -Aug2,1997, Book of Abstracts.
7. J. Macek and I. V. Hertel, J. Phys. B. 7, 2173 (1974).
8. M. Zuo, T. Y. Jiang, L. Vuskovic and B. Bederson, Phys. Rev. A41, 2489 (1990) and Z. Shi, C. H. Ying and L. Vuskovic, Phys. Rev. A54, 480 (1996).
9. P. W. Zetner, S. Trajmar, S. Wang, I. Kanik, , G.Csanak, R.E.H. Clark, J. Abdallah, Jr. and J. C. Nickel, J.Phys B to appear 1997.
10a. P. W. Zetner, S. Trajmar, I. Kanik, M. A. Khakoo, I Bray, D. Fursa, G.Csanak, R.E.H. Clark and G. Csanak (to be published).
10b. P. W. Zetner, S. Trajmar, I. Kanik, M. A. Khakoo, I Bray, D. Fursa, and G. Csanak (to be published).
11. S. Wang, S. Trajmar and P. W. Zetner, J. Phys. B. 27, 1613 (1994).
12. S. A. Kazantsev and J. C. Henoux, **Polarization Spectroscopy of Ionized** Gases, Kluwer Academic Publishers, London, 1995.

Report Number (14) LA-UR--97-4773
CONF-970710--

Publ. Date (11) 199802
Sponsor Code (18) DOE/DP, XF
UC Category (19) UC-700, DOE/ER

DOE